Removal of non-stationary noise by DCT based locally adaptive filtering

Vladimir V. Lukin[a], Dmitriy V. Fevralev[a], Sergey K. Abramov[a], Nikolay N. Ponomarenko[a], Sergey S. Krivenko[a], Oleksiy B. Pogrebnyak[b], Karen O. Egiazarian[c], Jaakko T. Astola[c], Igor Djurovič[d]

[a] National Aerospace University, 61070, Kharkov, Ukraine;
[b] Instituto Politecnico Nacional, Mexico, DF, Mexico;
[c] Tampere University of Technology, FIN 33101, Tampere, Finland;
[d] University of Montenegro, 81000, Podgorica, Montenegro

1. Introduction

Original images formed by different types of systems (digital cameras, remote sensing imagers, medical sensors, etc.) are noisy due to various phenomena like internal and external noise, transmission errors, limited time of received signal registration, operation principle of imaging system and so on. Because of these factors, image filtering has become an important stage of image pre-processing in many applications [1, 2]. Numerous filters intended for noise removal have been designed in recent fourty years. Since the end of sixtieth of the previous century, nonlinear filters gained popularity as a tool able to incorporate non-stationary nature of images as information processes (2D fields) [1-4]. Main attention in 70-th and 80-th was paid to nonlinear filters based on order statistics thoroughly analyzed and discussed in [2, 5, 6]. Their advantages and limitations were understood. In 90-th a lot of efforts were spent to getting around shortcomings of nonlinear non-adaptive filters. Investigations concentrated in two main directions: design of locally adaptive filters [7, 8] and transform based techniques [9, 10] although it is worth saying that there are methods that combine both approaches [11, 12]. Considerable attention was paid to incorporating knowledge on noise type and statitics for better removal of particular types of noise like impulse [13], speckle [14], etc.

Alongside with sufficient achievements in theory and practice, understanding of a fact that used models of noise were not adequate enough was coming steadily. Recall that typical simplified models are i.i.d. Gaussian noise with zero mean and constant variance often used in design of filters for optical images [1, 3] as well as i.i.d. pure multiplicative noise with unity mean and constant relative variance exploited in filtering of radar and ultrasound images [7, 11, 14]. Impulse noise that with equal probability can corrupt pixel values is considered often enough [2, 13], mixed noise models are quite common as well [1, 2].

However, recent investigations show that more complicated models of noise are worth applying to provide better adequateness to practice and, hence, to design and apply more efficient filters. To give a few examples, let us mention film-grain and other signal dependent noise models [12, 15, 16], spatially correlated noise models [17, 18], impulse burst and streak noises [19, 20], mixed multiplicative and additive noise model [21], etc. Note that often statistical and spatial correlation characteristics of noise or some part of them are not known in advance [21, 22].

If this takes place, one might follow two ways. One way is to apply a filter that in no way exploits a priori information on noise type and its statistical and spatial correlation characteritics. There are quite many examples of such filters: standard mean, median, α-trimmed mean, Wilcoxon, etc [2]. However, these filters often do not produce a desirable trade-off of basic properties (noise suppressionm edge-detai-texture preservation, removal of impulses, etc.) [2]

Another way is to exploit available a priori information and, if possible, get additional information from an image at hand and then to use it. In this connection, there exist blind methods for noise type determination [22]. If a noise type model is a priori known or correctly pre-determined, it becomes possible to estimate statistical characteristics for several given noise types like pure additive noise, speckle and multiplicative noise, special kinds of mixed noise (see [23] and refernces therein). Note that this can be done in a blind manner.

However, there are some practical limitations for this approach. First, currently existing version of the system for blind determination of noise type [22, 24]) does no allow recognizing all situations (noise types and their combinations) possible in practice. For example, till the moment such practically important types of noise as Poisson and film-grain ones cannot be recognized. Second, commonly it is

assumed that noise local variance has some dependence on local mean and this dependence is rather simple. Examples are Poisson and film-grain noises, pure multiplicative noise, etc. In all these cases, dependence of local variance on local mean is a monotonically increasing function [7, 10, 12]. However, there are practical situations when this dependence is not monotonic (one example will be given in the next Section). Moreover, local variance of noise can be also an unknown function of spatial coordinates (examples of such practical situations and reasons for arising noise with such properties are considered in [25]). Then, it becomes very difficult to decide how to "fit" a proper dependence (and is it possible to do this at all) and how to denoise such images.

It is worth mentioning here that if dependence of noise local variance on local mean or image coordinates (pixel indices) is a priori known or pre-determined, it is easy to perform image filtering that exploits such information about local variance. Examples of filters that are able to do this are sigma filter [26], its modifications [27], and DCT based filters [10]. Another, more complicated case happens when aforementioned dependence is unknown and cannot be determined. Below we pay main attention just to this case.

The task of non-stationary noise removal is not often and thoroughly considered in literature. Here we can mention the paper [28] as well as our recent papers [27, 29]. One of the reasons is complexity of this task. Complexity deals with the necessity to solve several particular problems. First, if a local transform based filtering (e.g., DCT based) is applied, one needs to set local thresholds in blocks and these local thresholds are to be adjusted to noise local statistics. It is not easy to obtain appropriately accurate blind estimates of noise statistics for entire image at hand even if noise is stationary [23, 30, 31]. Then, it is possible to expect that it is much more difficult to provide quite accurate local estimates of noise statistics in blocks or scanning windows of size 8x8 or 7x7. Second, it is desirable to adapt filter parameters to local properties of image content. Then, similar problem of providing reliable estimates or decisions for noisy data samples of small size arises.

These considerations and problems can be not very clear until more detailed analysis of noise properties is done and a structure of DCT-based local filtering is described. These analysis and description are given the next two Sections. Section 4 deals with main contribution of this paper, namely, property analysis for local estimates of noise standard deviation and image heterogeneity indicator. The latter is based on robust estimator of kurtosis (REK) [32, 33] applied in DCT domain [29]. We demonstrate that by analysis of REK histogram it is also possible to undertake decision is non-stationary noise spatially correlated or not. In Section 5, two local adaptive DCT based filters (hard switching one proposed in [29] and a new soft switching one) are described and studied by numerical simulations for a set of test images. Finally, we give some real life image processing examples in Section 6.

2. Initial assumptions concerning noise properties and problems of their local estimation

An initial assumption concerning non-stationary noise statistical properties is that in image homogeneous regions noise is quasi-Gaussian with zero mean but with unknown variance. The assumption of Gaussianity holds for many practical situations. Certainly, it holds for pure additive noise [1]. But this assumption is also valid for pure multiplicative noise in side-look aperture radars [7, 11] and in synthetic aperture radars with a large number of looks [10], Poisson noise except image regions with very low mean intensity [12, 34], component images of color, multispectral and hyperspectral remote sensing data [1, 35-37]. The only obvious declinations of noise statistics from being close to Gaussian noise are images formed by coherent imaging systems with one or few looks [10], [14].

Our second assumption is that noise variance in image homogeneous regions, in general, can be not constant but it changes slowly. For example, noise variance can change depending upon vertical or horizontal coordinate of an image as this happens for images formed by maritime radar where image horizontal coordinate is associated with distance (see details in [27]). At the same time, noise variance might have changes (variations) in neighborhood of edges. This can occur if noise contains few components (for example, additive and signal dependent). Thus, it is possible to rely on hypothesis of quasi-stationarity (HQS) of noise for image fragments (blocks) of rather small size but only if a given block does not correspond to image heterogeneity.

A third assumption is that, in general, non-stationary noise can be either spatially uncorrelated or spatially correlated. Strictly saying, it is not absolutely correct to consider correlation properties of non-stationary processes. But we are mainly interested in "close neighborhood" correlation, i.e., is it possible to consider values of noise in neighbor pixels independent or not. The reasons why it is important are threefold. First, spatially correlated noise is more hardly to suppress than uncorrelated one [7, 17, 18, 38]. Second, if noise is spatially correlated, this can influence accuracy of methods used for estimation of

noise statistics, both global [31] and local [29]. Third, for spatially correlated noise, one needs to have in advance or to obtain estimates of noise spatial correlation properties (e.g., normalized spatial spectrum) in order to improve noise suppression efficiency [18] by using operations similar or equivalent to pre-whitening. Note that such operations can lead to improvement of filter performance by 1...2 dB [18] in terms of both traditional metrics like MSE or PSNR and specialized metrics like PSNR-HVS that take into account peculiarities of human visual system [39, 40].

Therefore, we have come to several mutually dependent problems. At the very beginning, it is desirable to determine is noise spatially correlated or not. For this purpose, according to experience in [18] one might need to have quite many (about 1000 and, desirably, more) non-overlapping blocks that belong to image quasi-homogeneous regions. If such blocks are available it could be possible not only to determine is noise spatially correlated or not but also to estimate normalized spatial spectrum of noise. But how to select such blocks without knowledge of non-stationary noise local variance?

Here we should remind that under condition of known (predicted) local variance of noise $\sigma^2_{loc\,pr}$, discrimination of image homogeneous blocks is not a difficult task. It is enough to calculate local variance in a block as $\sigma^2_{loc\,bl} = \sum_{pq \in G} (I_{pq} - \overline{I}_{bl})^2 / (|G| - 1)$ where I_{pq} denotes a *pq*-th pixel of a considered image, $\overline{I}_{bl}$ is a given block mean, *G* is a set of pixels that belong to a given block, $|G|$ defines block size (expressed in number of pixels). Then a rule for discriminating image homogeneous blocks can be the following [18]: if $\sigma^2_{loc\,bl} \le \kappa \sigma^2_{loc\,pr}$, a block is homogeneous and vice versa. Here κ is a factor that depends upon noise statistics and block size. For 5x5 blocks (scanning windows), κ can be set in the limits 1.3...1.4 [18]. This can be done if there exists a known or pre-established dependence of $\sigma^2_{loc\,pr}$ on local mean $\overline{I}_{loc} : \sigma^2_{loc} = f(\overline{I}_{loc})$. Then, after calculating $\overline{I}_{bl}$ it is possible to calculate predicted local variance for a given block as $\sigma^2_{loc\,pr} = f(\overline{I}_{bl})$ and to use it for finding image homogeneous blocks. But if such prediction is impossible due to unknown statistics of non-stationary noise, one has to search for other methods for discriminating blocks. Below, in Section 4, we will show how this can be done.

Let us give an example of practical situation when prediction of noise statistics $\sigma^2_{loc} = f(\overline{I}_{loc})$ can be done hardly since this dependence possesses atypical properties. Consider a special test image (of size 512x512 pixels) that has 16 horizontal strips of width of 32 pixels. For each strip, the true values I^{tr}_{ij} are the same, i.e. constant and equal to 20 (for the leftmost strip), 30, 40,…, 170. This image has been corrupted by a signal-dependent noise of the following model of noisy image

$$I^n_{ij} = I^P_{ij} + n_{ij}, \tag{1}$$

where I^n_{ij} denotes an *ij*-th image pixel corrupted by Poisson noise with the true value equal to I^{tr}_{ij}, n_{ij} is zero mean i.i.d. additive Gaussian noise. This model simulates real life situation of noise in R, G, and B components of raw color images under assumption that variance of fluctuations $\sigma^2_{P\,ij} = I^{tr}_{ij}$ induced by Poisson noise for majority of image pixels is larger than variance of additive noise σ^2 considered to be constant [41]. In our simulations $\sigma^2 = 10$, therefore, the following conditions have been satisfied: $I^{tr}_{ij} - 3\sqrt{\sigma^2 + \sigma^2_{P\,ij}} > 0$ and $I^{tr}_{ij} + 3\sqrt{\sigma^2 + \sigma^2_{P\,ij}} < 255$ for any $I^{tr}_{ij} = 20, 30, ..., 170$ to keep 8-bit representation of data. Due to this, clipping effects in simulated noise are very seldom and their influence on further analysis is negligible. The noisy image is shown in Fig. 1,a.

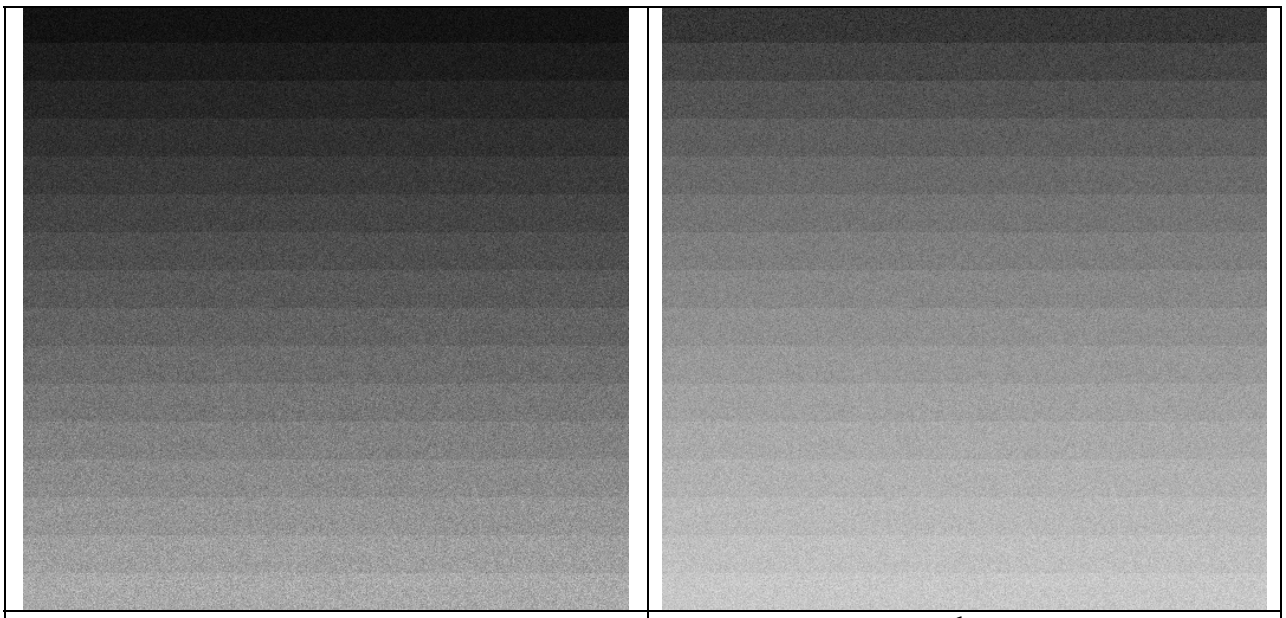

a b

Fig. 1. The original noisy test image (a) and this image after Gamma-correction ($\gamma = 0.6$) (b)

A typical operation used in digital cameras and other devices is Gamma correction [42]. In this case, a transformed (corrected) image is obtained as

$$I_{ij}^{\gamma} = f_{\gamma}(I_{ij}^{n}), \tag{2}$$

where $f_{\gamma}(.)$ is a monotonous function that defines gamma correction. Suppose that this function is of the form $I_{ij}^{\gamma} = 255(I_{ij}^{n}/255)^{\gamma} = 255^{1-\gamma}(I_{ij}^{n})^{\gamma}$ where the parameter $\gamma < 1$. The corrected test image $I_{ij}^{\gamma}, i = 1,...,512, j = 1,...,512$ is presented in Fig. 1,b ($\gamma = 0.6$).

Consider a scatter-plot of local estimates of variance obtained as $\sigma_{loc\,k}^2 = \sum_{ij \in G_k} (I_{pq} - \overline{I}_{bl\,k})^2 / (|G| - 1)$ where $\overline{I}_{bl\,k}$ denote a *k*-th block mean and corresponds to scatter-plot horizontal axis. The block size is 8x8. The blocks do not overlap. The scatter-plot for the original image $I_{ij}^{n}, i = 1,...,512, j = 1,...,512$ is presented in Fig. 2,a. As it is seen, there are 16 clusters that correspond to means for 16 strips of the test image. Cluster centers' positions can be well approximated by the straight line $\sigma_{loc}^2(I) = \sigma^2 + \sigma_P^2 = \sigma^2 + I^{tr}$ which is shown in Fig. 2,a.

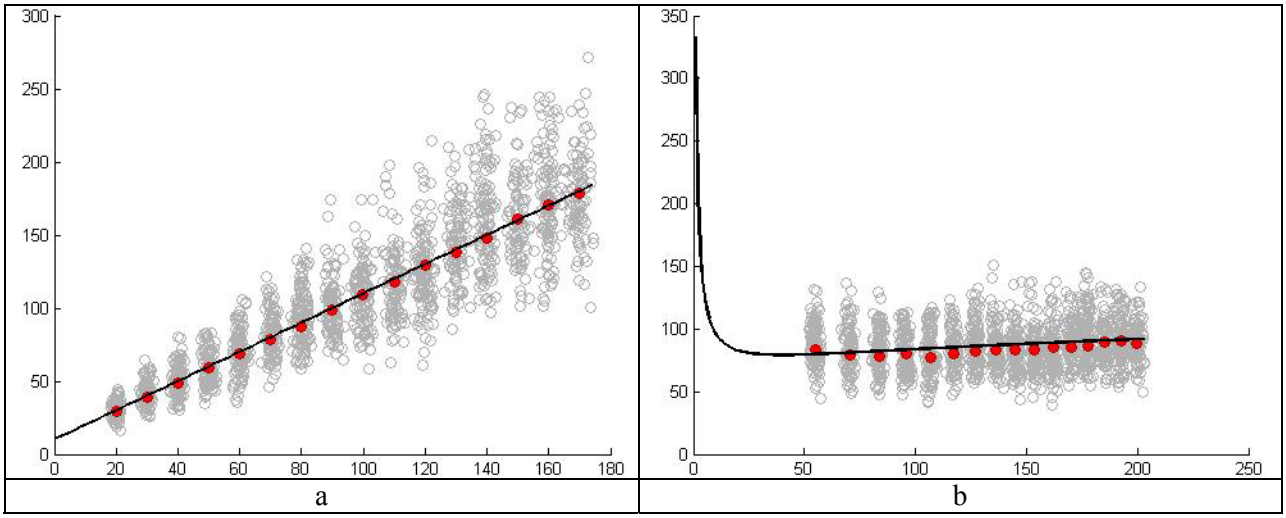

a b

Fig. 2. Scatter-plots of local estimates of variance for original noisy test image (a) and corrected image (b)

Assume that the noisy test image for a given pixel is represented as $I_{ij}^n = I_{ij}^{tr} + \Delta I_{ij}$ where ΔI_{ij} relates to both noise components (additive and Poissonian) and has zero mean and variance $\sigma_{ij}^2 = \sigma^2 + \sigma_{Pij}^2 = \sigma^2 + I_{ij}^{tr}$. Then, if $\sigma_{ij} << I_{ij}^{tr}$ and $f_\gamma(.)$ is a monotonous smooth function, it is possible to obtain $I_{ij}^\gamma \approx 255^{1-\gamma}(I_{ij}^{tr} + \Delta I_{ij})^\gamma = 255^{1-\gamma}((I_{ij}^{tr})^\gamma + \gamma(I_{ij}^{tr})^{\gamma-1}\Delta I_{ij})$. Thus, the mean of I_{ij}^γ is equal to $255^{1-\gamma}(I_{ij}^{tr})^\gamma$ whilst its variance is $\sigma_\gamma^2(I_{ij}^{tr}) \approx 255^{2-2\gamma}\gamma^2(I_{ij}^{tr})^{2\gamma-2}(\sigma^2 + I_{ij}^{tr})$ (the expressions are valid if $\sigma_{ij} << I_{ij}^{tr}$, otherwise more exact derivations are needed).

Let us ignore the positive constant term $255^{2-2\gamma}\gamma^2$ and analyze only the positive valued function $(I_{ij}^{tr})^{2\gamma-2}(\sigma^2 + I_{ij}^{tr})$. For the considered case of $\gamma < 1$ the factor $(I_{ij}^{tr})^{2\gamma-2}$ decreases with increasing of I_{ij}^{tr} whilst the factor $(\sigma^2 + I_{ij}^{tr})$ increases. Thus, depending upon γ and σ^2 the function $\sigma_\gamma^2(I_{ij}^{tr})$ can be monotonically increasing, monotonically decreasing or having maximum. The first case is typical for many types of images. The latter two cases are specific but they can also take place in practice. Let us demonstrate one of them for the considered test image. Consider $\gamma = 0.6$. The scatter-plot of local variance estimates for the corrected image $I_{ij}^\gamma, i = 1,...,512, j = 1,...,512$ is presented in Fig. 2,b. As seen, the means for strips have changed and are approximately equal to $255^{1-\gamma}(I_{ij}^{tr})^\gamma$. Sixteen clusters remained but their centers are now approximately positioned on the curve $\sigma_\gamma^2(I_{ij}^{tr}) = 255^{2-2\gamma}\gamma^2(I_{ij}^{tr})^{2\gamma-2}(\sigma^2 + I_{ij}^{tr})$ presented at the same plot.

The obtained results reveal, at least, two things. First, for images at hand that have been obtained by subjecting some original data to unknown transformations or to transformations of a known type with unknown parameters, the dependence $\sigma_{loc}^2 = f(I_{loc})$ can be not only monotonously increasing as it happens often but also decreasing or having a local extremum. Second, if one tries to fit some curve to an obtained scatter-plot (as this is done in a robust manner according to several already proposed approaches [21, 41]) it is necessary to use, at least, second order polynomials $\sigma_{loc}^2 = a_0 + b_0 I_{loc} + c_0 I_{loc}^2$ where a_0, b_0, c_0 are polynomial coefficients and $a_0 \geq 0$ in order to provide non-negative values of local variance for $I_{loc} = 0$. Coefficients b_0 and c_0 can be arbitrary, both negative and positive. While fitting a curve, it is also necessary to keep in mind that $\sigma_{loc}^2 = a_0 + b_0 I_{loc} + c_0 I_{loc}^2$ should be non-negative for all range of I_{loc}. To our opinion, these recommendations can be helpful in future research to be held for solving the task of blind estimation of dependence $\sigma_{loc}^2 = f(I_{loc})$ for real life images.

3. Structure of DCT-based local adaptive filtering

Let us rely on filtering based on DCT for locally adaptive removal of non-stationary noise. DCT based filtering is a good choice for our purpose because of several reasons. To understand them, let us recall basic steps and principles of DCT based filtering. First, it is carried out for an entire image in blocks-wise manner. The most typical case is the use of fixed size blocks (e.g., 8x8 [10, 11]) although block size and shape can be adapted as well [12]. Due to filtering in blocks, the method is well adapted to local quasi-stationarity of non-stationary noise. Second, DCT based filtering is carried out in four main stages:

1) performing forward DCT in each block with obtaining spectral coefficients $D(k,l,n,m)$ where indices *k,l* relate to DCT (spectral) coefficients and indices *n,m* denote a position (coordinates) of the left upper corner of an image block;
2) obtaining a set of thresholded spectral coefficients $D_T(k,l,n,m)$ by comparing absolute values of $D(k,l,n,m)$ to local thresholds $T(k,l,n,m)$ that , in general, can depend on all four indices, i.e. on block position and, respectively, local noise statistics as well as on spatial frequencies defined by indices *k,l*;
3) applying inverse DCT to the set of $D_T(k,l,n,m)$;
4) averaging the obtained filtered values for each image pixel if overlapping blocks are used.

This procedure of filtering allows adapting to local image content by remaining those spectral coefficients that are large enough by absolute values and, most likely, correspond to image information component. Note that DCT is one of the best decorrelation transforms approaching to Karhunen-Loeve transform. At the same time, proper setting of local thresholds for each block produces noise suppression and provides opportunity to adapt to spatial correlation of noise if this information is available. The use of overlapping blocks leads to considerable improvement of filtering performance in terms of PSNR (up to

2...3 dB) but it results in more computations in comparison to image processing in non-overlapping blocks [43].

As seen, the key item in DCT based filtering is a threshold setting. Since DCT is a linear orthogonal transform, each spectral coefficient $D(k,l,n,m) = D_I(k,l,n,m) + D_n(k,l,n,m)$ where $D_I(k,l,n,m)$ corresponds to true image and $D_n(k,l,n,m)$ to noise in a block defined by its left upper corner coordinates *n* and *m*. If one uses hard thersholding for which $D_T(k,l,n,m) = 0 \, if \, |D(k,l,n,m)| < T(k,l,n,m)$, then both positive and negative effects are provided. Suppose that $|D_I(k,l,n,m) + D_n(k,l,n,m)| < T(k,l,n,m)$. Then, assigning zero value to a given spectral coefficient $D(k,l,n,m)$ leads to "killing" the component $D_n(k,l,n,m)$ and this is a positive effect. Simultaneously zero value is, in fact, assigned to $D_I(k,l,n,m)$ and this introduces distortions into filtered image. Thus, thresholding has both positive and negative outcomes. Within a given block, variance of removed noise $\sigma^2_{remov}(n,m)$ is proportional to the following sum $\sum_{k=1}^{8}\sum_{l=1}^{8} D_n^2(k,l,n,m)\delta(k,l,n,m)$ where $\delta(k,l,n,m) = 1 if |D(k,l,n,m)| < T(k,l,n,m)$ and $\delta(k,l,n,m) = 0$ otherwise. Similarly, variance of introduced distortions $\sigma^2_{dist}(n,m)$ is proportional to $\sum_{k=1}^{8}\sum_{l=1}^{8} D_I^2(k,l,n,m)\delta(k,l,n,m)$. Moreover, some noise is remained and its variance $\sigma^2_{rem}(n,m)$ is proportional to $\sum_{k=1}^{8}\sum_{l=1}^{8} D_n^2(k,l,n,m)(1-\delta(k,l,n,m))$. This means that threshold increase leads to increase of $\sigma^2_{remov}(n,m)$, decrease of $\sigma^2_{rem}(n,m)$ (both effects are positive), but $\sigma^2_{dist}(n,m)$ increases (this effect is negative).

Theoretically, threshold setting for each block can be formulated as a task of minimization of the sum $\sigma^2_{rem}(n,m) + \sigma^2_{dist}(n,m)$, but practically it has not been solved yet since for each spectral component one has only the sum $D(k,l,n,m) = D_I(k,l,n,m) + D_n(k,l,n,m)$ but not each term of this sum separately. Because of this, in practice $T(k,l,n,m)$ is commonly set proportional to local standard deviation of noise as $\beta\sigma(k,l,n,m)$ where β is a proportion factor.

Several practical situations are possible. If one deals with i.i.d. additive Gaussian noise with a priori known variance σ^2_{add}, the threshold can be set fixed as $T = \beta\sigma_{add}$. If it is known that noise is additive, i.i.d., with PDF close to Gaussian and its variance $\hat{\sigma}^2_{add}$ is pre-estimated, then one can use fixed threshold $T = \beta\hat{\sigma}_{add}$ under assumption that the estimate $\hat{\sigma}^2_{add}$ is accurate enough. If noise is pure multiplicative and spatially uncorrelated with a priori known or pre-estimated variances σ^2_{μ}, $\hat{\sigma}^2_{\mu}$, respectively, then the threshold becomes to be locally adaptive: $T(n,m) = \beta\sigma_{\mu}\overline{I}(n,m)$ or $T(n,m) = \beta\hat{\sigma}_{\mu}\overline{I}(n,m)$ since it is needed to estimate (calculate) local mean $\overline{I}(n,m)$ for each block. Note that here $\sigma_{\mu}\overline{I}(n,m)$ or $\hat{\sigma}_{\mu}\overline{I}(n,m)$ are, in fact, estimates of noise standard deviation in an *nm*-th block $\hat{\sigma}_{loc}(n,m)$. In more generalized case of spatially uncorrelated noise and a priori known dependence $\sigma^2_{loc} = f(I_{loc})$, local threshold is to be set as $T(n,m) = \beta\sqrt{f(\overline{I}(n,m))}$ where $\sqrt{f(\overline{I}(n,m))}$ serves as an estimate of noise standard deviation in a given block.

In all these cases of spatially uncorrelated noise, local threshold depends only upon block coordinates defined by *n* and *m*. If noise is spatially correlated with a priori known normalized DCT power spectrum $W_{norm}(k,l)$ (supposed to be independent on spatial coordinates), local threshold becomes also dependent on indices *k* and *l* that relate to DCT components (frequencies). Then, for each block the threshold $T(n,m)$ as determined above for each particular noise type is also multiplied by $\sqrt{W_{norm}(k,l)}$ [18]. Hence, in general case, it becomes a function of four indices: *k*, *l*, *n*, and *m*.

The parameter β is commonly set fixed and approximately equal to 2.6 [10, 18, 43]. Such choice is motivated by the fact that for most images and noise characteristics it provides peak signal-to-noise ratio (PSNR) close to maximally reachable. More exactly, optimal β that provides maximal PSNR can

slightly deviate from 2.6. Optimal β is slightly larger than 2.6 for images with comparatively simple structure (i.e., for images that do not contain a lot of texture, small details and sharp high contrast edges) and if noise level is high enough (i.e., if PSNR for original noisy image is relatively small). On the contrary, optimal β slightly smaller than 2.6 can take place for highly textural images and/or if noise level is small enough. Moreover, analysis carried out in the paper [11] shows that for textural regions it is reasonable to set β about 2.2. In fact, setting β smaller than 2.6 is also reasonable for other types of image heterogeneous fragments like edge and detail neighborhoods. Below, for simplicity, we mainly concentrate on considering fixed β equal to 2.6 but take aforementioned observations into account.

Summarizing analysis and properties of DCT based filtering given above, it is possible to conclude the following:

1) DCT based filtering is a denoising tool that allows adapting to different types of noise by setting a proper local threshold under assumption that one has a "good" prediction or estimation of noise local standard deviation $\hat{\sigma}_{loc}(n,m)$;

2) Then, a local threshold can be set directly proportional to this local estimate of noise standard deviation $\hat{\sigma}_{loc}(n,m)$ where proportionality factor β is recommended to be fixed and equal to 2.6;

3) If noise is spatially correlated, the situation ones deals with is more complicated; it becomes necessary to adapt not only to noise standard deviation but also to spatial correlation properties of noise;

4) If requirements to image filtering time are not very strict, it is reasonable to perform filtering in overlapping blocks since it produces considerable improvement of processed image quality.

These conclusions concerning DCT based denoising main properties lead to necessity of solving several practical tasks in the considered situation of image corruption by non-stationary noise with hardly predicted and/or hardly estimated statistical and spatial correlation characteristics:

1) How to undertake a decision is noise spatially correlated or spatially uncorrelated?

2) If noise is spatially uncorrelated, how to estimate noise local standard deviation, what is accuracy of such estimates, is it appropriate and what to do if it is not appropriate?

3) If noise is spatially correlated, how to estimate noise standard deviation and spectral correlation characteristics of noise, what is accuracy of such estimates, is it appropriate for practice and what to do if it is not appropriate?

Below we mainly address first two questions and provide some useful information for answering the third question in future.

4. Local scale estimation and heterogeneity indication

4.1. Local variance estimation for spatially uncorrelated noise

To partly answer questions 2) and 3), one needs a method for estimating noise local standard deviation for an image at hand. Some initial imagination about methods for local estimation of noise standard deviation (variance) can be obtained from literature that addresses the issues of blind evaluation of noise variance in images [21, 23, 30, 31, 44] and locally adaptive filtering [7, 11, 45]. First, estimation can be carried out is spatial or spectral (wavelet, DCT) domains. Second, only in the case of pure additive i.i.d. noise, blind estimation can be performed by processing entire image [44]. In other cases, estimation is carried out by dividing an image into blocks or by searching and analyzing image homogeneous fragments [23]. Therefore, peculiarities of the estimates obtained in such blocks can be of interest in connection with our task.

Standard local estimates formed in blocks in spatial domain ($\sigma_c^2(n,m) = \sum_{p=n}^{n+7}\sum_{q=m}^{m+7}\left(I_{pq} - \overline{I}_{bl}(n,m)\right)^2 / 63$, $\overline{I}_{bl}(n,m)$ denotes mean for an *nm*-th block) are characterized by the following properties. For image homogeneous blocks, they are quite close to the true values of local variance $\sigma_{tr}^2(n,m) = \sum_{p=n}^{n+7}\sum_{q=m}^{m+7}\left(I_{pq} - I_{pq}^{tr}\right)^2 / 63$, but for image heterogeneous blocks the values of $\sigma_c^2(n,m)$ are considerably larger than the corresponding values of $\sigma_{tr}^2(n,m)$. On one hand, this means that the values of $\sigma_c(n,m)$ are unable to serve well for estimating local standard deviation of non-stationary noise [25]. On the other hand, these properties are effectively exploited in hard-switching locally adaptive filter design [7, 11, 45]. For any a priori known dependence $\sigma_{loc}^2 = f(I_{loc})$, it is possible

to estimate $\overline{I}_{bl}(n,m)$, to determine predicted $\sigma^2_{loc}(n,m) = f\left(\overline{I}_{bl}(n,m)\right)$ and to apply some noise suppressing filter (e.g., DCT-based filter) if $\sigma^2_c(n,m) \le \tau\sigma^2_{loc}(n,m)$ or good edge/detail preserving filter (e.g., sigma [26] or center weighted median [46] filters) if $\sigma^2_c(n,m) > \tau\sigma^2_{loc}(n,m)$ where τ is the parameter commonly set about 1.3. Details and particular examples of such design can be found in [11,45].

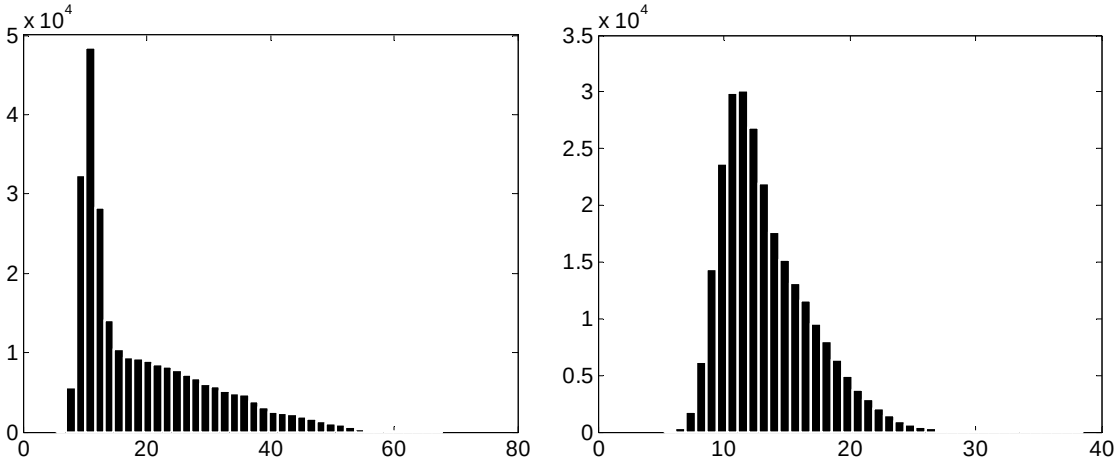

a b

Fig. 3. Histograms of $\hat{\sigma}_c(n,m)$ (a) and $\hat{\sigma}_{ort}(n,m)$ (b) for the image Barbara, $\sigma^2_{add} = 100$.

Peculiarities of the estimates $\sigma^2_c(n,m)$ discussed above are illustrated in Fig. 3,a for one of the standard test images, Barbara, corrupted by i.i.d. pure additive Gaussian naise with variance $\sigma^2_{add} = 100$. As it is seen, the values of $\hat{\sigma}_c(n,m)$ for the considered noisy image can be by 5...6 times larger than σ_{add}. This shows that estimates $\hat{\sigma}_c(n,m)$ are very sensitive to image heterogeneities.

Another approach presumes estimation of noise standard deviation in spectral domain. The basic assumption put behind the corresponding techniques [9, 30, 44] is that after applying an efficient data decorrelating orthogonal transform, true image information is concentrated in a rather small percentage of spectral components with large absolute values whilst remainder spectral components mainly relate to noise. Thus, by some processing of their statistics that should be robust to outlier data it is possible to estimate noise standard deviation.

Consider first the case of spatially uncorrelated noise. One possible way to carry out estimation of local standard deviation of noise in a block is to obtain a local estimate as

$$\hat{\sigma}_{ort}(n,m) = 1.483\,\mathrm{med}\left\{\left|D(k,l,n,m)\right|, k = 0,...,7; l = 0,...,7 \text{ except } k = 0 \wedge l = 0\right\}, \quad (3)$$

where med{.} denotes a sample median. In fact, the operation (3) exploits known median of absolute deviations (MAD) estimate [2] to characterize sample data scale under assumption of Gaussian contaminated distribution. The histogram of $\hat{\sigma}_{ort}(n,m)$ is presented in Fig. 3,b. As seen, this estimate of noise standard deviation is more accurate than $\hat{\sigma}_c(n,m)$, its largest values are only 2…3 times larger than σ_{add}. Certainly, such accuracy cannot be considered good. But one should keep in mind that for data samples of small size (63 elements for the considered case) it is theoretically impossible to provide high accuracy of scale estimation. Recall that we rely on hypothesis of local quasi-stationarity of noise.

More detailed analysis of $\hat{\sigma}_{ort}(n,m)$ [25, 29] has shown that the values of $\hat{\sigma}_{ort}(n,m)$ sufficiently larger than those of $\sigma_{tr}(n,m)$ are observed in image heterogeneous regions. Thus, although the estimates $\hat{\sigma}_{ort}(n,m)$ are more accurate and robust with respect to image content than $\hat{\sigma}_c(n,m)$,

they are not as accurate as desirable (appropriate). A question is what is desirable? An answer is that a local estimate ($\hat{\sigma}_{ort}(n,m)$ or some other one) should be within the limits $[0.8\sigma_{\mu}(n,m);1.2\sigma_{\mu}(n,m)]$. This requirement indirectly follows from results presented in the paper [47]. As it follows from analysis of the histogram in Fig. 3,b, this requirement is not satisfied for quite many local estimates $\hat{\sigma}_{ort}(n,m)$. This means that the problem of designing accurate local estimators of noise standard deviation remains. Unfortunately, till the moment we are unable to propose a better solution to this problem.

Here it is worth mentioning that if an estimate $\hat{\sigma}_{ort}(n,m)$ is considerably larger than $\sigma_{tr}(n,m)$ and $\hat{\sigma}_{ort}(n,m)$ is used for local threshold calculation as $T(n,m)=2.6\hat{\sigma}_{ort}(n,m)$, then oversmoothing for the corresponding *nm*-th block can be observed. One way how to partly get around this shortcoming will be described in the next Section.

4.2. Local variance estimation for spatially correlated noise

Estimation of local variance for spatially correlated noise is even more difficult than for spatially uncorrelated. One reason is that additional ambiguity appears. It concerns spatial correlation characteristics that can be also unknown. There can be different practical situations and, respectively, different initial assumptions on spatial correlation characteristics of noise. A most general assumption is that only few neighboring pixels have high correlation of noise and there is practically no periodicity and correlation of noise for pixels that are located quite far away from each other. In other words, one can suppose that a 2D spatial auto correlation function (ACF) looks something like that one presented in Fig. 4 where there is a main lobe which is not delta-function and ACF side lobes are quite small. At the same time, other parameters of ACF can in practice vary. For example, main lobe widths for horizontal and vertical cross-sections of the main lobe can be equal or different as the latter holds for the ACF in Fig. 4.

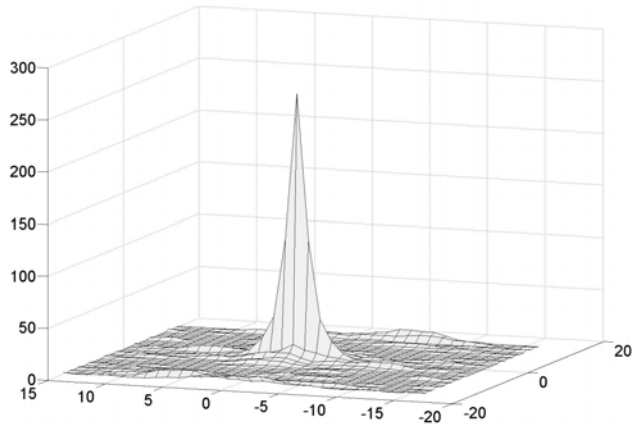

Fig. 4. An example of 2-D ACF of noise obtained for 32x32 homogeneous fragment of L-band SAR image

Another feature of spatially correlated noise is that its spatial correlation properties can be practically constant for an entire image or they can be different for different fragments. For example, spatial correlation properties of noise can vary as a function of distance from an imaging system to a sensed surface (object). This case is, probably, the most complicated for designing methods intended for blind image processing (filtering, edge detection, reconstruction).

Thus, we would like to stress basic difficulties of analyzing and processing images corrupted by spatially correlated noise. These difficulties are the following. First, there is a wide variety of possible models and variants to simulate such noise. Second, image processing methods should perform well enough for certain limits of variation of such models' parameters and these limits are not always known a priori. Third, if, at least, noise type is a priori known and spatial correlation characteristics are spatially invariant, this simplifies the task. But for non-stationary noise with a priori unknown dependence $\sigma^2_{loc}=f(I_{loc})$ the task of synthesizing efficient image processing methods becomes extremely difficult. Probably, these are the reasons why a number of papers devoted to processing images corrupted by spatially correlated noise is very limited.

Our goal in this subsection is to give information concerning the behavior and properties of local estimates of noise standard deviation $\hat{\sigma}_{ort}(n,m)$ and $\hat{\sigma}_c(n,m)$. Their more detailed analysis can be found in our paper [31].

Again, let's start from considering image homogeneous regions. A common general tendency for both $\hat{\sigma}_c(n,m)$ and $\hat{\sigma}_{ort}(n,m)$ is that, on the average, they decrease if 2D ACF main lobe width increases [31]. However, there is a difference between the estimates $\hat{\sigma}_c(n,m)$ and $\hat{\sigma}_{ort}(n,m)$. The difference is that the estimates $\hat{\sigma}_c(n,m)$ decrease only slightly especially if a used block (scanning window) size is considerably larger than the number of pixels that correspond to the 2D ACF main lobe. On the contrary, the estimates $\hat{\sigma}_{ort}(n,m)$ can, on the average, decrease considerably, by several times [31], especially if a 2D ACF main lobe is rather wide. This difference can be observed from comparison of histograms presented in Figures 5 and 3. Note that main attention in comparison should be paid to positions of distribution modes that are formed by the estimates obtained for image homogeneous blocks. Thus, essential difference in modes' coordinates for the distributions of the estimates $\hat{\sigma}_c(n,m)$ and $\hat{\sigma}_{ort}(n,m)$ can be one indicator that a given image is corrupted by spatially correlated noise. This observation needs special thorough study for designing practically applicable algorithms for identification of images corrupted by spatially correlated noise.

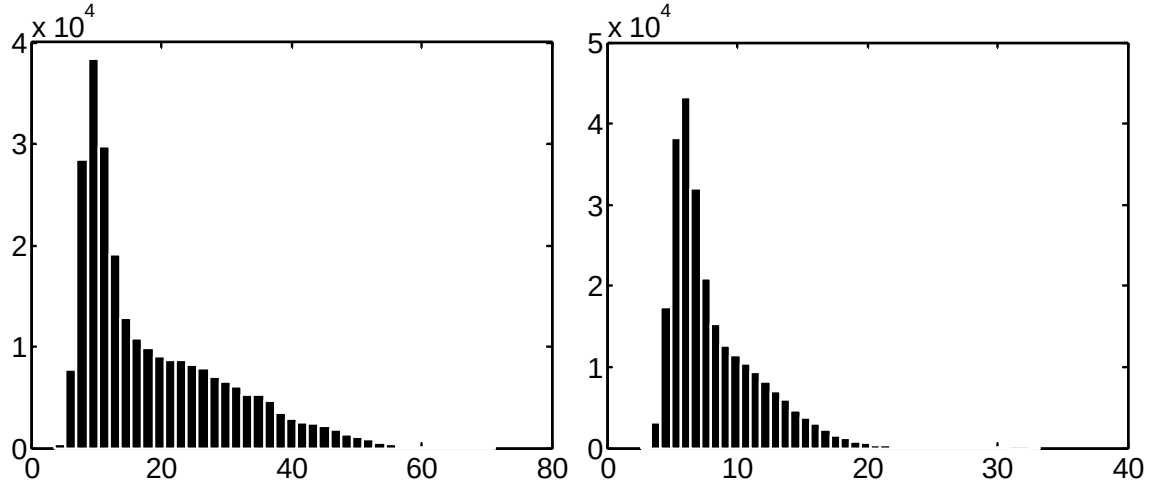

a b

Fig. 5. Histograms of estimates $\hat{\sigma}_c(n,m)$ (a) and $\hat{\sigma}_{ort}(n,m)$ (b) for the image Barbara corrupted by spatially correlated noise with $\sigma^2_{add} = 100$

However, in estimation of local standard deviations of non-stationary spatially correlated noise one deals not only with image homogeneous blocks considered above but also with image heterogeneous blocks. For the latter type of blocks, the situation is very similar to the case of spatially uncorrelated noise discussed in subsection 4.1. Image heterogeneity leads to the estimates $\hat{\sigma}_c(n,m)$ and $\hat{\sigma}_{ort}(n,m)$ that are both larger than $\hat{\sigma}_{tr}(n,m)$ for the corresponding blocks. This effect appears itself as heavy right hand tails of distribution in both histograms presented in Fig. 5. As earlier (see Fig 3), this tail is heavier for the estimates $\hat{\sigma}_c(n,m)$ that are more sensitive to heterogeneities.

The main conclusion that follows from the analysis carried out in this subsection is that both estimates $\hat{\sigma}_c(n,m)$ and $\hat{\sigma}_{ort}(n,m)$ produce very inaccurate evaluations of local standard deviation in the case of non-stationary spatially correlated noise. It is then difficult to expect that the corresponding DCT based filtering will be efficient. To prove this, let us present output MSE values for two image filtering cases. The first is filtering a test image corrupted by spatially correlated noise under condition that both noise variance and spatial spectrum are a priori exactly known (MSE_{akn}). Another is filtering the same image when there is no a priori information on noise statistics and spectral correlation by setting $T(n,m) = 2.6\hat{\sigma}_{ort}(n,m)$ (MSE_{unk}). Consider a simplest case of pure additive spatially correlated noise with variance 100. The obtained values of MSE are presented in Table 1. Besides, in this Table we present the

values of MSE_{uncorr} for the case of filtering spatially uncorrelated noise with the same variance $\sigma^2_{add} = 100$ and fixed threshold $T(n,m) = 2.6\sigma_{add} = 26$.

Table 1. MSE values for the compared filtering cases

Image	Lena	Barbara	Baboon	Peppers	Goldhill
MSE_{akn}	33.1	37.2	65.4	33.8	49.6
MSE_{unk}	54.2	74.7	189.5	74.0	82.3
MSE_{uncorr}	19.2	23.9	59.0	22.2	30.7

As it can be seen from comparisons, MSE_{uncorr} values are considerably smaller than MSE_{akn} for all tested images. This means that, in general, it is more difficult to remove spatially correlated noise than uncorrelated one even in conditions of having full a priori information on noise characteristics at disposal. In turn, the values MSE_{unk} are larger than the corresponding values MSE_{unk}. This is due to several reasons. The first reason is inaccurate estimation of local standard deviation of noise whereas the second reason is that spatial correlation of noise has not been taken into account in filtering when thresholds were set as $T(n,m) = 2.6\hat{\sigma}_{ort}(n,m)$. Both undersmoothing effects have been observed in image homogeneous regions and oversmoothing has taken place in heterogeneous regions of output images. Since the image Babbon is the most textured image between the considered test ones, the results for it were the worst. MSE_{unk} occurred to be larger than $\sigma^2_{add} = 100$ for the input image. In other words, filtering has led to worse quality of the filtered image than the quality of input image.

The presented examples and simulation data demonstrate the following:

1) For spatially correlated noise, the problem of estimating its local standard deviation is even more complex than for spatially correlated noise and its solving needs special study;
2) To improve filtering performance, it is strongly desirable to know or to pre-estimate noise normalized spectrum; if one has correctly identified image homogeneous regions, this task can be solved by using the method proposed in [18];
3) The problems of identifying images corrupted by spatially correlated noise and detecting image heterogeneous regions in them remain.

4.3. Heterogeneity indication in images corrupted by non-stationary noise

Recall that our purpose is to discriminate image homogeneous and heterogeneous blocks without having a priori information what are true values of local standard deviation of noise in these blocks. Recently, a method for this has been proposed [29]. This method is based on the known fact that there are differences in statistics of orthogonal transform coefficients for noise and image content. In particular, in several papers (see, e.g., [48], statistics of wavelet coefficients has been considered. It has been demonstrated that the distribution of wavelet coefficients is composite where two components – Gaussian $\rho_G(x)$ and Laplacian $\rho_L(x)$ – are both present: $\rho_w(x) = p\rho_G(x) + (1-p)\rho_L(x)$. Here p denotes the distribution parameter that is quite large for noisy images that contain many image homogeneous regions and not a lot of details and texture. The component probability density function (PDF) $\rho_G(x)$ is characterized by zero mean and variance σ^2_G proportional to noise variance, the PDF component $\rho_L(x)$ also has zero mean and variance σ^2_L that depends upon spatial spectrum properties of image information content. Usually the following inequality holds: $\sigma^2_L > \sigma^2_G$.

Similar effects are observed in entire image [30] and in blocks for the distribution $\rho_{DCT}(x)$ of DCT coefficients $D(k,l,n,m), k = 0,...,7, l = 0,...,7$ (the DC coefficient $D(0,0,n,m)$ was excluded from consideration). If a block belongs to image homogeneous region, the parameter p approaches to unity, otherwise p is smaller. The Laplacian component of the distribution has heavier tail than Gaussian one and it mainly relates to information content of images.

Thus, to detect heterogeneous blocks, one is able to apply some test on non-Gaussianity of $D(k,l,n,m), k = 0,...,7, l = 0,...,7$. For this purpose, it has been proposed in [29] to use a parameter $E^{DCT}(n,m)$ that is similar to percentile coefficient of kurtosis (PCK) [49] that for 8x8 blocks is defined as:

$$E^{DCT}(n,m) = (D^{(58)}(n,m) - D^{(6)}(n,m)) / (D^{(48)}(n,m) - D^{(16)}(n,m)) \quad (4)$$

where $D^{(t)}(n,m)$ denotes a *t*-th order statistic (DC coefficient is excluded from consideration). As it is seen, $E^{DCT}(n,m)$ does not require information on standard deviation of noise to be calculated.

Recall that PCK can be used for characterizing tail heaviness for non-Gaussian distributions [49]. As so, PCK or its modifications like (4) can serve our goal of discriminating homogeneous and heterogeneous blocks of images. The only thing one should remember is that distribution of DCT coefficients in an image homogeneous block is close to Gaussian only if noise is spatially uncorrelated. Therefore, let us consider this case from the beginning and then see what happens if noise is spatially correlated.

As it follows from properties of order statistics, nominator in (4) is always not less than denominator and, thus, $E^{DCT}(n,m)$ is larger than unity. If distribution of DCT coefficients in a block is Gaussian, the mean of $E^{DCT}(n,m)$ is approximately equal to 2.1. Therefore, setting a threshold T_{DCT} larger than 2.1 can be used for detection of image heterogeneous blocks as

$$Det(n,m) = \begin{cases} 1, if\ E^{DCT}(n,m) \geq T_{DCT} \\ 0, if\ E^{DCT}(n,m) < T_{DCT} \end{cases} . \quad (5)$$

It is usual for detectors [6, 7] that setting a larger threshold results in less reliable detection but smaller probability of false alarm and vice versa. Because of this, some trade-off should be found. We recommend setting T_{DCT} approximately equal to 2.5.

Note that (5) is not the edge detection algorithm in strict sense. It is image heterogeneous block detector to be used for further filtering. Its performance can be illustrated by the following example. Fig. 6,a shows the noise-free test image Cameraman. Then, additive i.i.d. noise with variance equal to 100 has been added to the image and the detector (5) has been applied. The obtained map of $Det(n,m)$ is represented in Fig. 6,b where black color pixels correspond to zeroes and white color ones relate to unities. As it is seen, edges and other heterogeneities are detected quite well and encountered by wide "strips" (in this sense, (5) is not a good edge detector). Certainly, some low contrast object edges and textures are not detected and few false detections are present.

a b

Fig. 6. Original noise-free Cameraman image of size 512x512 pixels (a) and heterogeneity detection map (of size 505x505 pixels) for noisy image (b)

It can be also interesting to see how the distribution of $E^{DCT}(n,m)$ looks like. We have determined it for the image Cameraman corrupted by pure additive noise (Fig. 7,a) and by Poisson noise (Fig. 7,b). In both cases, distributions have maximums (modes) for $E^{DCT}(n,m)$ of about 2.1 and heavy right hand tails that correspond to image heterogeneous blocks.

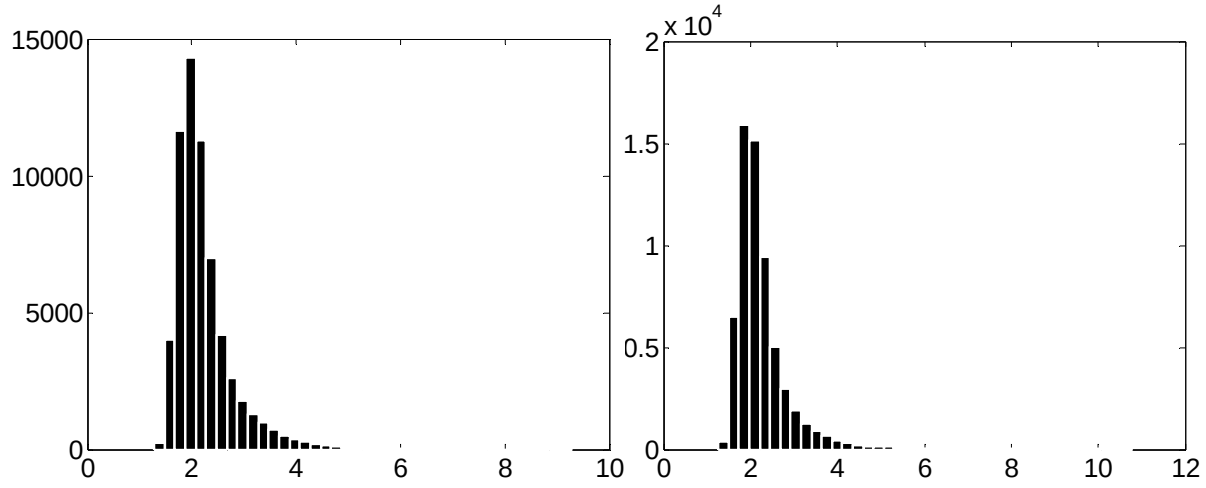

a b

Fig. 7. Histograms of distributions for $E^{DCT}(n,m)$ for the test image Cameraman corrupted by spatially uncorrelated additive (a) and Poisson (b) noise

Consider now the case of spatially correlated noise. Even for image homogeneous blocks the distribution of DCT coefficients is not Gaussian and its shape depends upon spatial spectrum of noise. For image heterogeneous blocks there are few large amplitude components that additionally make distribution more heavier tailed. Examples of distributions of $E^{DCT}(n,m)$ for spatially correlated noise are presented in Fig. 8 for pure additive and Poisson noises.

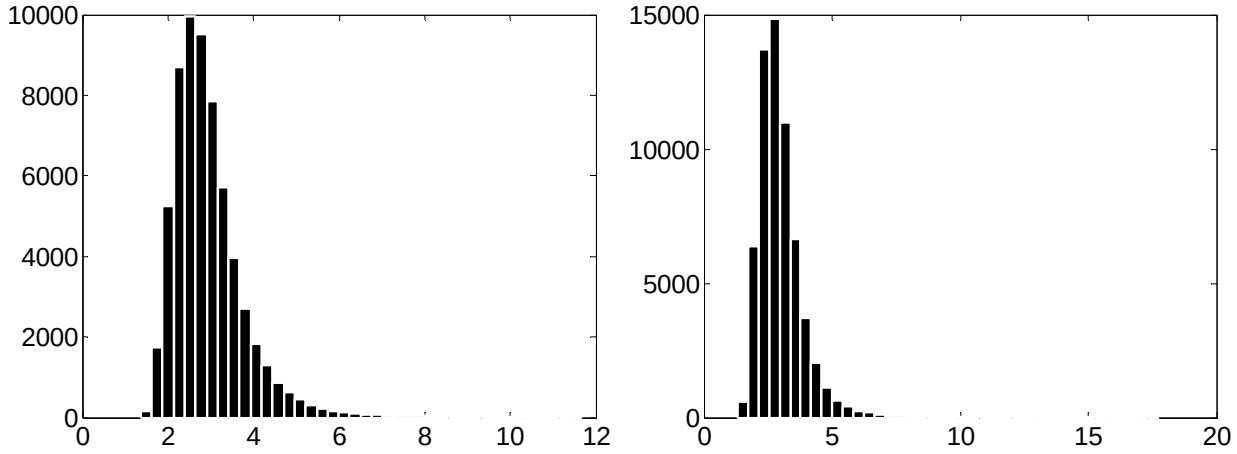

a b

Fig. 8. Histograms of distributions of $E^{DCT}(n,m)$ for the test image Cameraman corrupted by spatially correlated additive (a) and spatially correlated Poisson (b) noise

Again, both histograms have right hand heavy tails that are formed by $E^{DCT}(n,m)$ observed for image heterogeneous blocks. Mode values for these distributions have moved to larger values in comparison to the corresponding histograms in Fig. 7. Positions of histogram modes can be a feature that allows discriminating the cases of spatially correlated and uncorrelated noise.

This idea needs: a) checking for different test images, noise types, variances and spatial correlation characteristics; b) an algorithm for estimation a distribution mode (histogram maximum argument); c) a decision rule to decide is noise spatially uncorrelated or not. Fortunately, the algorithm for distribution mode estimation exists. Moreover, we have proposed several of them [31, 50, 51]. The most advanced one is described in the latest paper [31] and is based on minimal inter-quantile differences (distances) and their polynomial approximation for obtaining a more accurate estimate.

Thus, it is possible to get an estimate $\hat{E}_{\text{mod}}$. A simple decision rule might be comparison of $\hat{E}_{\text{mod}}$ to a threshold E_{thr}. Let us analyze simulation results to get imagination about this threshold, at least,

approximately. For this purpose, spatially uncorrelated and spatially correlated noises have been simulated and added to five test images. Spatially correlated noise has been simulated as i.i.d. noise subjected to filtering by 3x3 mean filter, then its variance has been adjusted to have a desired variance. Clearly, spatially correlated noise can be simulated by many other methods. However, our goal was to obtain initial results and to see what happens for different images and noise types, is there some difference between values of $\hat{E}_{\text{mod}}$ for spatially correlated and uncorrelated noise. The obtained data are presented in Table 2.

Table 2. The estimates $\hat{E}_{\text{mod}}$ for the test images corrupted by different types of noise

Image	Lena	Barbara	Baboon	Peppers	Goldhill
Type of noise	$\hat{E}_{\text{mod}}$	$\hat{E}_{\text{mod}}$	$\hat{E}_{\text{mod}}$	$\hat{E}_{\text{mod}}$	$\hat{E}_{\text{mod}}$
Additive spatially uncorrelated	2.0052	2.0713	2.1412	1.9992	2.0370
Poisson spatially uncorrelated	2.0030	2.0706	2.1224	1.9963	2.0397
Additive spatially correlated	2.6831	2.8944	2.4770	2.4163	2.6389

Analysis of data in Table 2 shows that for spatially uncorrelated noise (additive and Poisson) the values $\hat{E}_{\text{mod}}$ are smaller than for images corrupted by spatially correlated noise. At the same time, $\hat{E}_{\text{mod}}$ depends upon an image. For images with larger complexity (more texture, edges, details), the values $\hat{E}_{\text{mod}}$ are larger (consider the data for the image Baboon) than for less complex images like Lena and Peppers. It is possible to set a threshold E_{thr} the use of which allows discriminating spatially correlated and uncorrelated noise cases. It seems reasonable to set it about 2.2. However, this task needs more thorough study to give a final answer.

5. Local adaptive filtering of non-stationary noise

In this Section, we consider the case of filtering non-stationary spatially uncorrelated noise supposing that it has been identified by the algorithm proposed in the previous subsection. Recall that now we have the algorithm (3) for local estimation of noise standard deviation (although not appropriately accurate) and the algorithm (5) for discrimination of image homogeneous and heterogeneous blocks (although misclassifications for this algorithm are possible). We also know that the estimates $\hat{\sigma}_{ort}(n,m)$ are larger than $\hat{\sigma}_{tr}(n,m)$ for image heterogeneous blocks and, if the local threshold is set as $T(n,m) = 2.6\hat{\sigma}_{DCT}(n,m)$, this leads to image oversmoothing. Thus, the idea proposed in [29] is to apply one more mechanism of local adaptation, i.e. to adapt not only to local scale of data in a given block but also to local content. The idea is to set some smaller local threshold than $T(n,m) = 2.6\hat{\sigma}_{DCT}(n,m)$ to avoid oversmoothing. Then, a simple algorithm of such adaptation is

$$T(n.m) = \begin{cases} 2.6\hat{\sigma}_{DCT}(n,m), if\ Det(n,m) = 0 \\ \beta_{het}\hat{\sigma}_{DCT}(n.m), if\ Det(n,m) = 1 \end{cases}, \quad (6)$$

where β_{het} is the parameter used for filtering image heterogeneous blocks and a value of this parameter should be not larger than 2.6. However, a question is what is optimal or, at least, reasonable value of β_{het}?

To answer this question we have carried out a special study [29] using not only the standard quantitative criterion of filter performance (PSNR) but also parameters that characterize the visual quality of filtered images, namely, PSNR-HVS [39], PSNR-HVS-M [40], and MSSIM [52]. These results are presented below in Tables 3 and 4. Analysis of these data shows the following. Due to hard switching adaptation (5), filter performance has been sufficiently improved according to all considered criteria. A reasonable practical choice seems to be β_{het}=1.1. Further decreasing of β_{het} leads to increase of MSE and decrease of PSNR-HVS, PSNR-HVS-M, and MSSIM.

Table 3. Performance characteristics for the test image Barbara corrupted by pure additive noise with variance 100

β_{het}	2.6	2.3	2.0	1.7	1.4	1.1
MSE	33.95	31.40	29.36	27.95	**27.31**	27.46

PSNR-HVS	30.70	30.96	31.18	31.34	31.42	**31.43**
PSNR-HVS-M	34.22	34.48	34.71	34.87	34.95	**34.98**
MSSIM	0.980	0.981	0.982	0.982	**0.983**	**0.983**

Table 4. Performance characteristics for the test image Lena corrupted by pure additive noise with variance 100

β_{het}	2.6	2.3	2.0	1.7	1.4	1.1
MSE	24.25	23.36	22.56	21.95	21.56	**21.46**
PSNR-HVS	31.49	31.62	31.74	31.84	31.89	**31.91**
PSNR-HVS-M	34.52	34.58	34.69	34.75	34.79	**34.81**
MSSIM	0.977	0.977	0.978	0.978	0.978	**0.978**

However, these are only preliminary conclusions done for two particular images, one type of noise and one particular value of its variance. Because of this, we have also carried out simulations for Poisson spatially uncorrelated noise. The obtained results (output MSE) are given in Table 5 for five test images. As it is seen, again we have improvements and they are the largest for β_{het}=1.1 for four of five images (the best results are marked as Bold). However, for the test image Baboon the filter performance is not good even for β_{het}=1.1 and smaller β_{het} is needed to provide smaller output MSE. However, even in this case the output MSE occurs to be only slightly smaller than input MSE (132.9). This shows that it is difficult to expect good performance of the proposed adaptive filter for highly textural images.

Table 5. Output MSE values for five test images corrupted by Poisson spatially uncorrelated noise

β_{het}	2.6	2.3	2.0	1.7	1.4	1.1
BABOON	186.6	174.2	161.7	150.2	140.6	132.9
GOLDHILL	43.2	41.7	40.2	38.8	37.7	**37.0**
PEPPERS	28.1	27.3	26.6	25.9	25.4	**25.1**
BARBARA	36.1	33.5	31.5	30.0	**29.4**	29.6
LENA	24.2	23.4	22.6	22.0	21.6	**21.5**

According to (5), only two values of β can be used in setting a local threshold, namely one equal to 2.6 and another, smaller than 2.6 (e.g., 1.1). It is a simple practical solution but it is not the only possible option. For example, it is possible to set β as some function of $E^{DCT}(n,m)$. An initial requirement is that this function should decrease if $E^{DCT}(n,m)$ increases. Since it is difficult to provide a theoretically optimal function, we decided to carry out preliminary study using a simple exponential function

$$\beta(n,m) = 2.6(2/E^{DCT}(n,m))^{\alpha}, \quad (7)$$

where α>0 is a parameter. The ratio $2/E^{DCT}(n,m)$ is selected for providing $\beta(n,m)$ of about 2.6 for image homogeneous blocks where mean of $E^{DCT}(n,m)$ is approximately equal to 2.

Simulations have been carried out for two images (Lena and Baboon) that considerably differ from each other in their content (percentage of heterogeneous regions). Pure additive spatially uncorrelated noise with variance 100 was considered. The obtained output MSEs are presented in Table 6. It is interesting that the tendencies for the considered images are contradictory. Whilst for the image Lena α about 1.5 is quasi-optimal (minimal output MSE is produced) and further increasing of α leads to increase of output MSE, for the image Baboon optimum is not reached even for α=4.0. Thus, practical choice is problematic and it can be a topic for future research. As initial practical recommendation, we can propose to use α=3.0. Note that for the image Baboon the output MSE in this case is sufficiently smaller than for the hard switching locally adaptive filter (see data in Table 5).

Table 6. Output MSE for locally adaptive filter based on (7)

α	1.5	2.0	2.5	3.0	3.5	4.0
Lena	20.7	20.8	21.4	22.2	23.5	24.6
Baboon	114.1	103.0	93.5	87.2	82.0	78.9

Let us give an example of applying the designed locally adaptive filter based on (7) to the image Goldhill corrupted by Poisson spatially uncorrelated noise. The original noise free image is shown in Fig. 9,a and the noisy image is demonstrated in Fig. 9,b (pure additive noise with variance 100). The field of the parameter $E^{DCT}(n,m)$ is presented in Fig. 9,c. As it is seen, this parameter locates the fragments with image heterogeneities. The processed image is represented in Fig. 9,d. Noise is considerably removed whilst edges and fine details are preserved well enough.

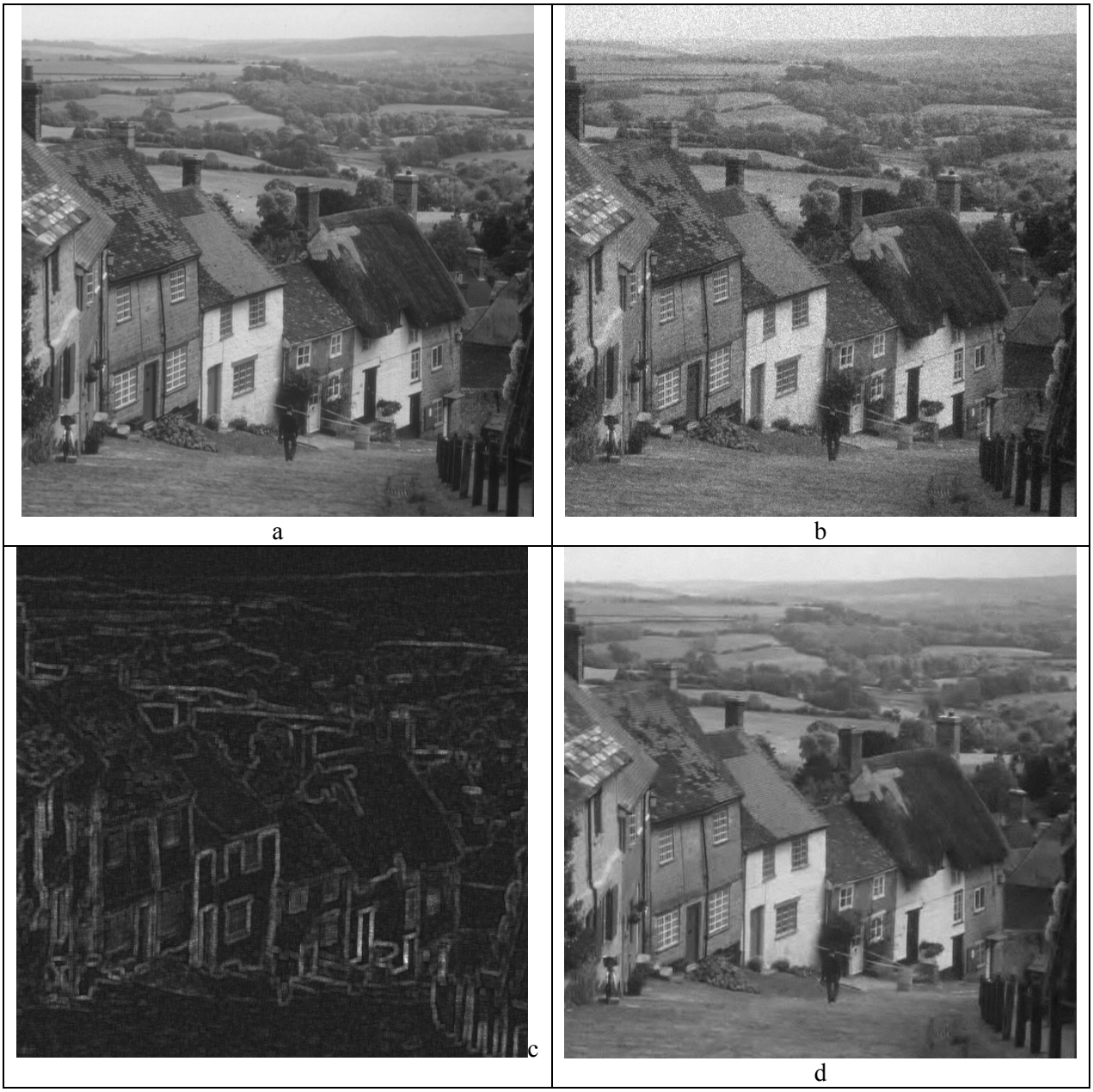

Fig. 9. Noise free image Goldhill (a), its noisy version (b), visualized field of $E^{DCT}(n,m)$ (lighter pixels correspond to larger values) (c), and the filtered image (d)

6. Examples for real life images

Let us present two examples of applying the designed locally adaptive DCT filter to real life images. The first example is a sub-band 224 image of hyperspectral AVIRIS data Lunar Lake [53] (Fig. 10,a). It is corrupted by noise that is visually seen. The visualized field of $E^{DCT}(n,m)$ is presented in Fig. 10,b. It indicates positions of image heterogeneous regions well. Analysis of the histogram of $E^{DCT}(n,m)$

shows that percentage of image heterogeneous blocks is not too large. Histogram maximum $\hat{E}_{\text{mod}}$ is about 1.97. This indicates that noise is spatially uncorrelated. The field of the estimates $\hat{\sigma}_{ort}(n,m)$ is visualized in Fig. 10,c. Its analysis shows that it has larger values in image heterogeneous regions. Finally, the filtered image is represented in Fig. 10,d. Useful information is preserved and noise is sufficiently suppressed.

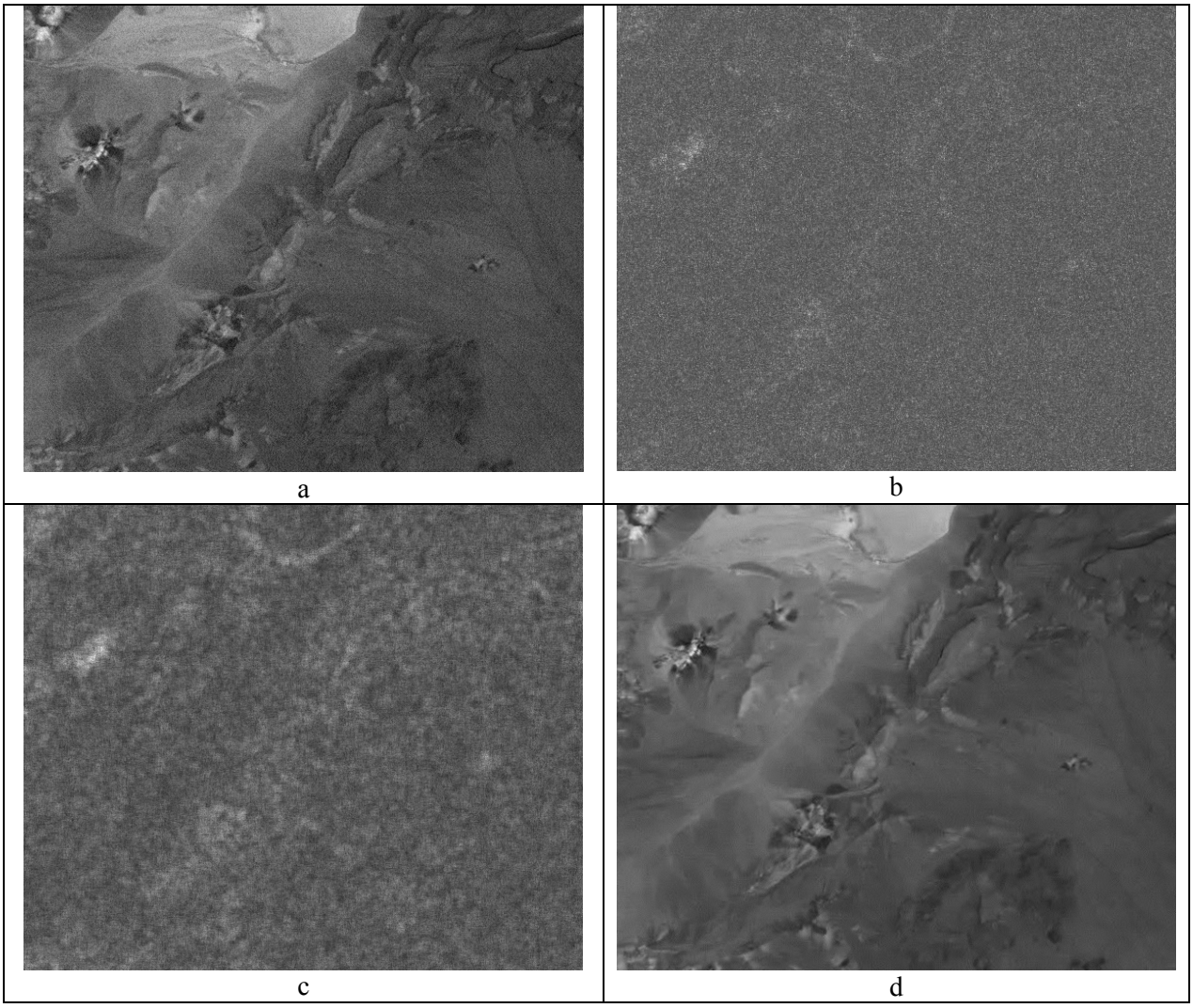

Fig. 10. Noisy sub-band image Lunar Lake (a), visualized field of $E^{DCT}(n,m)$ (lighter pixels correspond to more homogeneous regions) (b), visualized estimated of noise standard deviation $\hat{\sigma}_{ort}(n,m)$ (c), and the filtered image (d)

One more practical situation when noise is not stationary takes place in side look radar imaging [21]. In general, the dominant component of noise is multiplicative but additive noise is present as well. The paper [21] describes the way how to evaluate statistics of both components but here we would like to show how image filtering can be performed without such evaluation. First, we have found $\hat{E}_{\text{mod}}$ for the K_a-band real life radar image presented in Fig. 11,a. $\hat{E}_{\text{mod}}$ is equal to 2.32. Thus, noise seems to be spatially correlated although it is possible to expect that spatial correlation is not large. The filtered image is presented in Fig. 11,d and its quality is quite high. For spatially correlated noise we used $\beta(n,m)$ $=2.6(\hat{E}_{\text{mod}} / E^{DCT}(n,m))^{\alpha}$.

It is also interesting to see at behavior of visualized estimated of noise standard deviation $\hat{\sigma}_{ort}(n,m)$ (Fig. 11,c). As it is seen, the values $\hat{\sigma}_{ort}(n,m)$ are larger (lighter in the visualized map) for image regions with larger local mean. This indicates that noise is signal dependent. This conclusion is in agreement with traditional assumption on mainly multiplicative nature of noise. Fig. 11,b represents the

visualized field of $E^{DCT}(n,m)$ values. As it is seen, large (light) pixels indicate discontinuities and texture in the original noisy image.

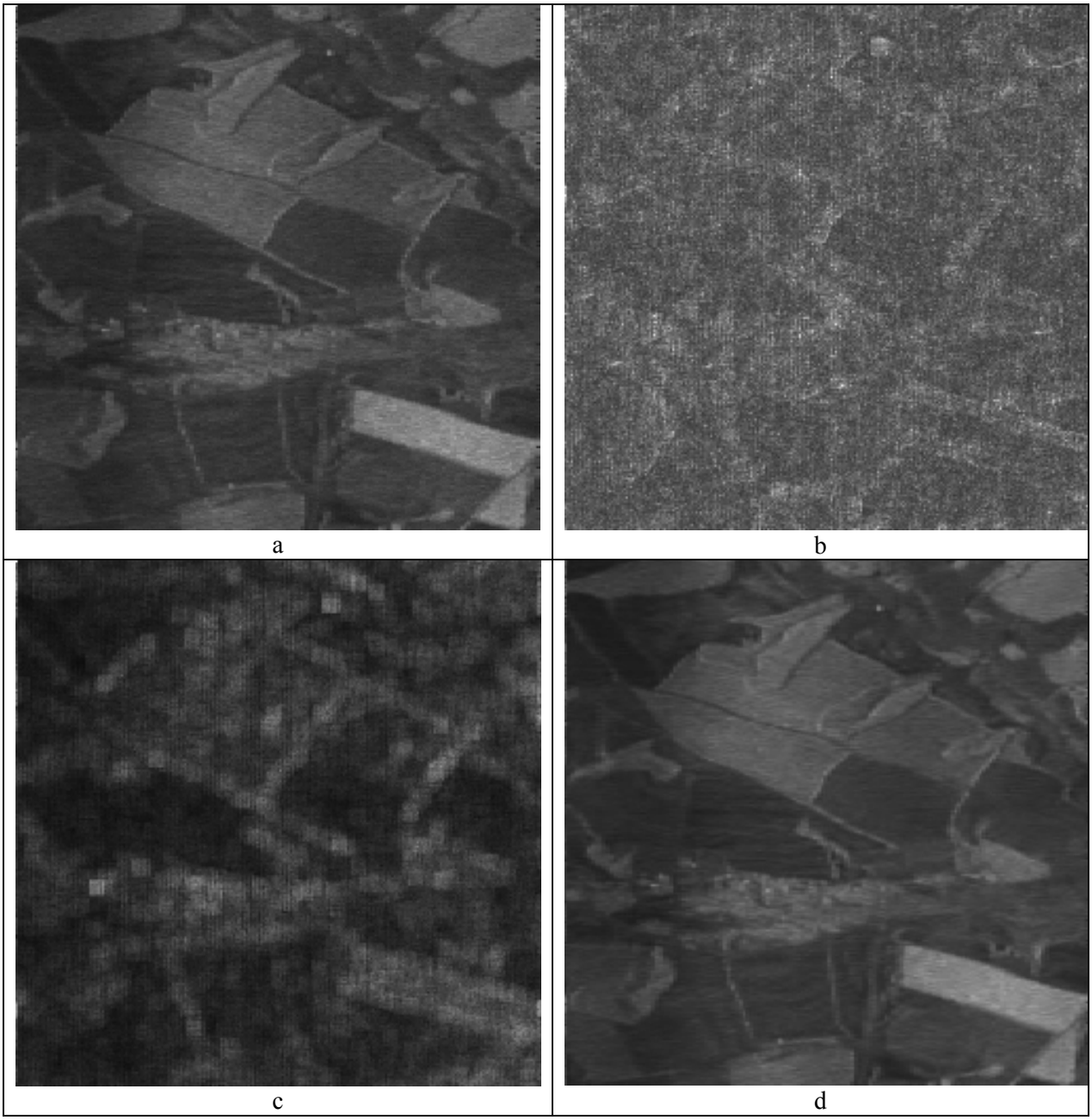

Fig. 11. Noisy K_a-band Radar image (a), visualized field of $E^{DCT}(n,m)$ (lighter pixels correspond to more homogeneous regions) (b), visualized estimated of noise standard deviation $\hat{\sigma}_{ort}(n,m)$ (c), and the filtered image (d)

The presented results show that the designed filter can be successfully applied to real life images.

Conclusions and future work

An important practical task of removing non-stationary noise with a priori unknown statistical and spatial correlation characteristics is addressed in this paper. It is demonstrated that it can be solved on basis of locally adaptive DCT based filtering. The first local adaptation mechanism is blind estimation of noise standard deviation in image blocks of fixed size. The second mechanism of local adaptation deals with discrimination of locally active (heterogeneous) and passive (homogeneous) image regions on basis of the introduced local parameter $E^{DCT}(n,m)$ and its use in setting a local threshold. Besides, analysis of this parameter histogram allows discriminating the cases of spatially uncorrelated (simpler case) and correlated (more complex case) noise. The latter case requires additional studies in order to design a

method for estimating spatial (DCT) normalized spectrum that can be incorporated in frequency dependent threshold setting in order to further improve filtering performance.

References

1. K.N. Plataniotis, A.N. Venetsanopoulos, Color Image Processing and Applications, Springer-Verlag, NY, 2000.
2. J. Astola, P. Kuosmanen, Fundamentals of nonlinear digital filtering, CRC Press LLC, Boca Raton, USA, 1997.
3. W.K. Pratt, Digital Image Processing. Fourth Edition. NY, USA, Wiley-Interscience, 2007.
4. E.R. Davies, D. Charles, "Color Image Processing: Problems, Progress, and Perspectives", Chapter 11 in "Advances in Nonlinear Signal and Image Processing", USA: Hindawi, 2006, pp. 301-328.
5. Nonlinear Signal and Image Processing: Theory, Methods, and Applications (Electrical Engineering & Applied Signal Processing Series), Ed. by K. Barner and G. Arce, CRC Press, 2003, 560 p.
6. Pitas I., Venetsanopoulos A.N. Nonlinear Digital Filters: Principles and Applications. Boston (USA): Kluwer Academic Publisher, 1990, 321 p.
7. V. Melnik, "Nonlinear Locally Adaptive Techniques for Image Filtering and Restoration in Mixed Noise Environments", Thesis for the degree of Doctor of Technology, Tampere University of Technology, Tampere, Finland, 234 p., 2000, http://www.atilim.edu.tr/~roktem/Research/interests.htm.
8. L.P. Yaroslavsky, Local criteria and local adaptive filtering in image processing: a retrospective view, CD-ROM Proceedings of LNLA, Lausanne, Switzerland, Aug. 2008, 8 p.
9. S. Mallat, A Wavelet tour of signal processing, Academic Press, San Diego, 1998.
10. R. Oktem, K. Egiazarian, V. Lukin, N. Ponomarenko, O. Tsymbal, Locally Adaptive DCT Filtering for Signal-Dependent Noise Removal, EURASIP Journal on Advances in Signal Processing, Article ID 42472, 10 p., 2007.
11. Tsymbal O.V., Lukin V.V., Ponomarenko N.N., Zelensky A.A., Egiazarian K.O., Astola J.T., Three-state Locally Adaptive Texture Preserving Filter for Radar and Optical Image Processing, EURASIP Journal on Applied Signal Processing, No 8, pp. 1185-1204, May 2005.
12. A. Foi, Pointwise Shape-Adaptive DCT Image Filtering and Signal-Dependent Noise Estimation: Thesis for the degree of Doctor of Technology, Tampere University of Technology, Tampere, Finland, Dec. 2007.
13. Eng H.-L.,Ma K.-K., "Noise adaptive soft switching median filter", IEEE Trans. on Image Processing, vol. 10, No 2, p. 242–251, 2001.
14. J.S. Lee, J.H. Wen, T.I. Ainsworth, K.S. Chen, A.J. Chen, Improved Sigma Filter for Speckle Filtering of SAR Imagery, IEEE Transactions on Geoscience and Remote Sensing, Vol. 47, No 1, Jan. 2009, pp. 202-213.
15. R. Öktem and K. Egiazarian, Transform Domain Algorithm for Reducing the Effect of Film-Grain Noise in Image Compression, Electronic Letters, vol. 35, no. 21, pp. 1830-1831, 1999.
16. F. Argenti, G. Torricelli, L. Alparone, Signal dependent noise removal in the undecimated wavelet domain, Proceedings of ICASSP 2002, pp. 3293-3296, 2002.
17. Deergha R., Swamy M.N.S., Plotkin E., Adaptive filtering approaches for colour image and video restoration, IEE Proceedings on Vision, Image and Signal Processing, Vol. 150, No 3, pp. 168-177, 2003.
18. V. Lukin, N. Ponomarenko, K. Egiazarian, J. Astola, Adaptive DCT-based filtering of images corrupted by spatially correlated noise, Proc. SPIE Conference Image Processing: Algorithms and Systems VI, Vol. 6812, 12 p., 2008.
19. E. Abreu, M. Lightstone, S.K. Mitra, K. Arakawa, A new approach for the removal of impulse noise from highly corrupted images, IEEE Transactions on Image Processing, Vol. 6, No 5, pp. 1012-1025, 1996.
20. Koivisto P., Astola J., Lukin V., Melnik V., Tsymbal O. Removing Impulse Bursts from Images by Training Based Filtering, EURASIP Journal on Applied Signal Processing, Vol. 2003, No 3, 2003, pp. 223-237.
21. V.V. Lukin, N.N. Ponomarenko, S.K. Abramov, B. Vozel, K. Chehdi, J. Astola, Filtering of radar images based on blind evaluation of noise characteristics, Proceedings of Image and Signal Processing for Remote Sensing XIV, Cardiff, UK, Sept 2008, SPIE Vol. 7109, 12 p.
22. M.-P. Carton-Vandecandelaere, B. Vozel, L. Klaine, K. Chehdi, Application to Multispectral Images of a Blind Identification System for Blur, Additive, Multiplicative and Impulse Noises, Proceedings of EUSIPCO, Toulouse (France), Vol. III, pp. 283-286, 2002.
23. B. Vozel, S. Abramov, K. Chehdi, V. Lukin, N. Ponomarenko, M. Uss, Blind methods for noise evaluation in multi-component images, book chapter in "Multivariate image processing", ISTE Ltd, France, 2009.
24. B. Vozel, K. Chehdi, L. Klaine, V.V. Lukin, S.K. Abramov, Noise identification and estimation of its statistical parameters by using unsupervized variational classification, Proceedings of ICASSP, 2006, Toulouse, France, Vol. II, pp. 841-844.

25. V. Lukin, D. Fevralev, N. Ponomarenko, O. B. Pogrebnyak, K. Egiazarian, J. Astola, Local Adaptive Filtering of Images Corrupted by Nonstationary Noise, Proceedings of SPIE Conference "Image Processing: Algorithms and Systems VI", Vol. 7245, 12 p., San Jose, USA, 2009.
26. Lee J.-S. Digital Image Smoothing and the Sigma Filter, Comp. Vision, Graphics and Image Processing, 1983, Vol. 24, pp. 255-269.
27. Lukin V.V., Zelensky A.A., Ponomarenko N.N., Kurekin A.A., Astola J.T., Koivisto P.T. Modified Sigma Filter with Improved Noise Suppression Efficiency and Spike Removal Ability, Proceedings of the 6-th Intern. Workshop on Intelligent Signal Processing and Communication Systems, Melbourne (Australia), 1998, pp. 849-853.
28. T. Rabie, Robust Estimation Approach to Blind Denoising, IEEE Transactions on Image Processing, Vol. 14, No 11, Nov. 2005, pp. 1755-1766.
29. N. Ponomarenko, D. Fevralev, A. Roenko, S. Krivenko, V. Lukin, I. Djurovič, Edge Detection and Filtering of Images Corrupted by Nonstationary Noise Using Robust Statistics, Proceedings of CADSM2009, Feb. 2009, Svalyava, Ukraine, pp. 129-136.
30. Ponomarenko N.N., Lukin V.V., Abramov S.K., Egiazarian K.O., Astola J.T. Blind evaluation of additive noise variance in textured images by nonlinear processing of block DCT coefficients, Proceedings of International Conference "Image Processing: Algorithms and Systems II", Santa Clara, CA, USA, SPIE Vol. 5014, 2003, pp. 178-189.
31. V. Lukin, S. Abramov, B. Vozel, K. Chehdi, J. Astola, Segmentation-based method for blind evaluation of noise variance in images, SPIE Journal on Applied Remote Sensing, Vol. 2, Aug. 2008, 15 p. (open access paper)
32. A. Roenko, V. Lukin, S. Abramov, I. Djurovič, Adaptation of sample myriad tunable parameter to characteristics of SαS distribution, Proceedings of MMET, Odessa, Ukraine, June 2008, pp. 418-420.
33. Suoranta R. "Amplitude domain approach to digital filtering. Theory and applications of L-filters", Doctor of Technology Thesis, Espoo: Technical Research Centre of Finland, 1995, 199 p.
34. V. V. Lukin, D. V. Fevralev, S. K. Abramov, S. Peltonen, J. Astola, Adaptive DCT-based 1-D filtering of Poisson and mixed Poisson and impulsive noise, CD ROM Proceedings of LNLA, Switzerland, August 2008, 8 p.
35. V.V. Lukin, O.V. Tsymbal, B. Vozel, K. Chehdi, Processing multichannel radar images by modified vector sigma filter for edge detection enhancement, Proceedings of ICASSP, 2006, Vol. II, pp 833-836.
36. B. Aiazzi, L. Alparone, A. Barducci, S. Baronti, P. Marcoionni, I. Pippi, M. Selva, Noise modelling and estimation of hyperspectral data from airborne imaging spectrometers, Annals of Geophysics, Vol. 49, Feb. 2006, No 1, pp. 1-9.
37. A. Barducci, D. Guzzi, P. Marcoinni, and I. Pippi, "CHRIS-Proba performance evaluation: signal-to-noise ratio, instrument efficiency and data quality from acquisitions over San Rossore (Italy) test site", Proceedings of the 3-rd ESA CHRIS/Proba Workshop, Italy, 11 p., March 2005.
38. Lukin V.V., Melnik V.P., Pogrebniak A.B., Zelensky A.A., Saarinen K.P., Astola J.T., Digital adaptive robust algorithms for radar image filtering, Journal of Electronic Imaging, 5(3), pp. 410-421, 1996.
39. K. Egiazarian, J. Astola, N. Ponomarenko, V. Lukin, F. Battisti, M. Carli, New full-reference quality metrics based on HVS, CD-ROM Proceedings of the Second International Workshop on Video Processing and Quality Metrics, Scottsdale, USA, 2006, 4 p.
40. N. Ponomarenko, F. Battisti, K. Egiazarian, M. Carli, J Astola, V. Lukin, Metrics Performance Comparison for Color Image Database, Proceedings of Fourth International Workshop on Video Processing and Quality Metrics (VPQM), Jan. 2009, Scottsdale, USA, 6 p.
41. Foi A., M. Trimeche, Katkovnik V., Egiazarian K. Practical Poissonian-Gaussian Noise Modeling and Fitting for Single Image Raw Data, IEEE Transactions on Image Processing, Vol. 17, No 10, 2007, pp. 1737-1754.
42. Farid H., Blind inverse gamma correction, IEEE Transactions on Image Processing, Vol. 10, Oct. 2001, pp. 1428-1433.
43. V.V. Lukin, R. Oktem, N. Ponomarenko, K. Egiazarian, Image filtering based on discrete cosine transform, Telecommunications and Radio Engineering, Vol. 66, No 18, pp. 1685-1701, 2007.
44. L. Sendur, I.W. Selesnick, "Bivariate shrinkage with local variance estimation," IEEE Signal Processing Letters, Vol. 9, No 12, 438-441 (2002) (see also http://taco.polv.edu/WaveletSoftware/index.html)
45. Melnik V.P., Lukin V.V., Zelensky A.A., Astola J.T., Kuosmanen P., Local Activity Indicators: Analysis and Application to Hard-Switching Adaptive Filtering of Images, Optical Engineering Journal, Vol. 40, No 8, pp. 1441-1455,2001.
46. Sun T., Gabbouj M., Neuvo Y. Center weighted median filters: some properties and their applications in image processing, Signal Processing, Vol. 35, No 3, pp. 213-229, 1994.
47. Abramov S.K., Lukin V.V., Ponomarenko N.N., Egiazarian K.O., Pogrebnyak O.B., Influence of multiplicative noise variance evaluation accuracy on MM-band SLAR image filtering efficiency,

Proceedings of the Fifth International Kharkov Symposium “Physics and Engineering of Millimeter and Sub-Millimeter Waves”, Kharkov, Ukraine, June 2004, Vol.1, pp. 250-252.
48. S. Chang, B. Yu, M. Vetterli, “Adaptive Wavelet Thresholding for Image Denoising and Compression”, IEEE Transactions on Image Processing, Vol. 9, Sept 2000, pp. 1522-1531.
49. Suoranta R. “Amplitude domain approach to digital filtering. Theory and applications of L-filters”, Doctor of Technology Thesis, Espoo: Technical Research Centre of Finland, 1995, 199 p.
50. V.V. Lukin, S.K. Abramov, A.A. Zelensky, J.T. Astola, Use of minimal inter-quantile distance estimation in image processing, Proceedings of SPIE Conference on Mathematics of Data/Image Pattern Recognition, Compression, and Encryption with Applications IX, SPIE Vol. 6315, San Diego, USA, 2006, 12 p.
51. Lukin V.V., Abramov S.K., Vozel B., Chehdi K. Improved minimal inter-quantile distance method for blind estimation of noise variance in images, Proceedings of SPIE/EUROPTO Symposium on Satellite Remote Sensing, Florence, Italy, Sept 2007, 12 p.
52. Matthew Gaubatz, "Metrix MUX Visual Quality Assessment Package: MSE, PSNR, SSIM, MSSIM, VSNR, VIF, VIFP, UQI, IFC, NQM, WSNR, SNR", http://foulard.ece.cornell.edu/gaubatz/metrix_mux/
53. AVIRIS Home page, http://aviris.jpl.nasa.gov/, Accessed Jan 6, 2007.